DOI: 10.1534/genetics.110.118315

Comparative Transcriptome Analysis of the CO_2 Sensing Pathway Via Differential Expression of Carbonic Anhydrase in *Cryptococcus neoformans*

Min Su Kim,*[,1] Young-Joon Ko,*[,1] Shinae Maeng,* Anna Floyd,[†] Joseph Heitman[†] and Yong-Sun Bahn*[,2]

**Department of Biotechnology, Center for Fungal Pathogenesis, Yonsei University, Seoul 120-749, Korea and [†]Departments of Molecular Genetics and Microbiology, Medicine, and Pharmacology and Cancer Biology, Duke University Medical Center, Durham, North Carolina 27710*

Manuscript received April 29, 2010
Accepted for publication May 24, 2010

ABSTRACT

Carbon dioxide (CO_2) sensing and metabolism via carbonic anhydrases (CAs) play pivotal roles in survival and proliferation of pathogenic fungi infecting human hosts from natural environments due to the drastic difference in CO_2 levels. In *Cryptococcus neoformans*, which causes fatal fungal meningoencephalitis, the Can2 CA plays essential roles during both cellular growth in air and sexual differentiation of the pathogen. However the signaling networks downstream of Can2 are largely unknown. To address this question, the present study employed comparative transcriptome DNA microarray analysis of a *C. neoformans* strain in which *CAN2* expression is artificially controlled by the *CTR4* (copper transporter) promoter. The P_{CTR4}*::CAN2* strain showed growth defects in a CO_2-dependent manner when *CAN2* was repressed but resumed normal growth when *CAN2* was overexpressed. The Can2-dependent genes identified by the transcriptome analysis include *FAS1* (fatty acid synthase 1) and *GPB1* (G-protein β subunit), supporting the roles of Can2 in fatty acid biosynthesis and sexual differentiation. Cas3, a capsular structure designer protein, was also discovered to be Can2-dependent and yet was not involved in CO_2-mediated capsule induction. Most notably, a majority of Can2-dependent genes were environmental stress-regulated (ESR) genes. Supporting this, the *CAN2* overexpression strain was hypersensitive to oxidative and genotoxic stress as well as antifungal drugs, such as polyene and azole drugs, potentially due to defective membrane integrity. Finally, an oxidative stress-responsive Atf1 transcription factor was also found to be Can2-dependent. Atf1 not only plays an important role in diverse stress responses, including thermotolerance and antifungal drug resistance, but also represses melanin and capsule production in *C. neoformans*. In conclusion, this study provides insights into the comprehensive signaling networks orchestrated by CA/CO_2-sensing pathways in pathogenic fungi.

CARBON dioxide (CO_2) sensing, transport, and metabolism are critical in survival, proliferation, and differentiation in diverse microbes, including pathogenic fungi (Bahn and Mühlschlegel 2006). Opportunistic fungal pathogens exposed to ambient air in a natural environmental setting must overcome dramatic changes in CO_2 levels during infection (150-fold change from 0.036 to 5%). In *Candida albicans*, which causes superficial and systemic candidiasis in immunocompromised patients, high CO_2 levels induce the morphological transition from yeast to hypha that is an important virulence attribute contributing to tissue adhesion and invasion of the pathogen (Sims 1986; Mock *et al.* 1990). Recently it has been reported that CO_2 sensing by *C. albicans* is mediated by adenylyl cyclase, which produces cAMP, thereby activating protein kinase A (PKA) to trigger filamentous growth (Klengel *et al.* 2005). Another striking example of fungal CO_2-mediated signaling has also been demonstrated in *Cryptococcus neoformans*, which causes fatal fungal meningoencephalitis in both immunocompetent and immunocompromised individuals. High CO_2 levels enhance antiphagocytic polysaccharide capsule production during infection (Granger *et al.* 1985; Vartivarian *et al.* 1993) and inhibit sexual differentiation by blocking cell–cell fusion via repression of pheromone production (Bahn *et al.* 2005).

During CO_2 sensing and metabolism, carbonic anhydrase (CA), a zinc-containing metalloenzyme, is the key enzyme that catalyzes hydration of CO_2 and produces bicarbonate (HCO_3^-) and a proton (H^+). Since the soluble form of CO_2, bicarbonate, is likely to be a key intracellular CO_2 signaling molecule as well as a substrate for diverse carboxylating enzymes essential for lipid, amino acid, and pyrimidine synthesis, CAs are

Supporting information is available online at http://www.genetics.org/cgi/content/full/genetics.110.118315/DC1.

[1]These authors contributed equally to this work.

[2]*Corresponding author:* Department of Biotechnology, Yonsei University, 134 Shinchon-dong, Seodaemun-gu, Seoul 120-749, Korea. E-mail: ysbahn@yonsei.ac.kr

considered to play pivotal roles in the metabolic process. CA is ubiquitously found in all organisms, catalyzing diverse cellular processes including carbon fixation in plants, and tumor development, respiration, pH and ion homeostasis, and electrical activity in the retinal and nervous systems in mammals (Bahn and Mühlschlegel 2006). The CA enzyme family can be broadly grouped into four classes: α-CA, β-CA, γ-CA, and δ-CA (for reviews, see Henry 1996; Tripp *et al.* 2001). The α-CAs are widely distributed in bacteria, plants, and mammals. In humans, 14 α-class CAs have been identified including four membrane-associated (IV, IX, XII, and XIV) and extracellularly secreted (VI) CAs. Particularly, CA IV and XIV were found to be extracellular membrane-bound CAs expressed in the lung and brain (Wang *et al.* 1997; Parkkila *et al.* 2001).

β-CAs are found in bacteria, algae, plants, and fungi, but not in mammals (Henry 1996; Watson *et al.* 2003). Fungal β-CA was first characterized in the nonpathogenic model yeast, *Saccharomyces cerevisiae*, called Nce103, and found to be essential for growth in ambient CO_2 levels (Gotz *et al.* 1999; Clark *et al.* 2004; Amoroso *et al.* 2005). The requirement of Nce103 for growth can be relieved by enriching air with 5% CO_2 (Amoroso *et al.* 2005), which appears to result in spontaneous hydration of CO_2 into bicarbonate. The role of fungal CA in pathogenic fungi has been recently uncovered in *C. albicans* and *C. neoformans* (Bahn *et al.* 2005; Klengel *et al.* 2005; Mogensen *et al.* 2006). *C. albicans* contains a single functional CA, called Nce103 (Klengel *et al.* 2005), whereas *C. neoformans* possesses two CAs, named Can1 and Can2, although the latter is the major form of CA (Bahn *et al.* 2005; Mogensen *et al.* 2006). Disruption of genes encoding Nce103 and Can2 causes growth arrest of *C. albicans* and *C. neoformans*, respectively, under ambient air conditions (Bahn *et al.* 2005; Klengel *et al.* 2005; Mogensen *et al.* 2006). Normal growth of those CA mutants can be restored by incubating them in either high CO_2 conditions or an animal host (Bahn *et al.* 2005; Klengel *et al.* 2005). Interestingly, these studies raised the hypothesis that CAs might be directly or indirectly involved in fungal CO_2 signaling pathways. In *C. albicans*, the activity of adenylyl cyclase (AC) to produce cAMP and thus activate the cAMP-signaling pathway is enhanced by bicarbonate (Klengel *et al.* 2005; Mogensen *et al.* 2006). In *C. neoformans*, the mating inhibition by high CO_2 can be partially reversed by mutation of the *CAN2* gene (Bahn *et al.* 2005). Therefore, fungal CA is not only crucial for cell survival and proliferation, but also mediates various CO_2-related signaling cascades that are important for virulence and differentiation of pathogenic fungi. On the basis of recent analysis of crystal structure of Can2 (Schlicker *et al.* 2009), Can2 belongs to the "plant-type" β-CA and carries a unique N-terminal extension consisting of four antiparallel α-helices. The N-terminal extension of Can2 appears to interact with the active site entrance of the dimer (Schlicker *et al.* 2009). Although lipid biosynthesis was found to be one of the essential cellular processes affected by mutation of the CA gene (Bahn *et al.* 2005), downstream genes and signaling networks regulated by CO_2 and CAs remained to be elucidated.

To elucidate downstream target genes of a signaling network, genome-wide comparative transcriptome analysis by using the wild-type (WT) strain and the corresponding mutant strain is normally employed. However, this type of comparative analysis is not appropriate for identifying target genes downstream of Can2 since the *can2*Δ deletion mutant exhibits severe growth defects under ambient air conditions, and growth restoration of the *can2*Δ mutant by enrichment with high CO_2 will bypass the requirement of Can2 by spontaneous hydration of CO_2 into bicarbonate (HCO_3^-). To circumvent this problem, we constructed a *C. neoformans* strain in which expression levels of the *CAN2* gene are artificially controlled by an alternative promoter system. For this purpose, we used the copper-regulated *CTR4* promoter system that has been successfully utilized to conditionally modulate expression levels of genes of interest (Ory *et al.* 2004; Chayakulkeeree *et al.* 2007). We employed this strain to elucidate its transcriptome patterns by DNA microarray to identify and characterize genes whose transcript levels are regulated directly or indirectly by Can2 in *C. neoformans*. This transcriptome analysis discovered a number of CA-dependent genes, including those involved in fatty acid biosynthesis (*FAS1*), organization of polysaccharide capsule (*CAS3*), and sexual differentiation (*GPB1*), although a majority of them do not have any known function. Furthermore, among the Can2-dependent genes, a number of environmental stress-response (ESR) genes and the oxidative stress-responsive Atf1 transcription factor were included, suggesting that differential CA expression could be correlated with stress-response regulation in *C. neoformans*. Therefore, this study not only elucidates CA-dependent genes on a genome-wide scale for the first time, but also provides further insights into the signaling network of CA/CO_2-sensing pathway in pathogenic fungi.

MATERIALS AND METHODS

Strains and media: The strains used in this study are listed in supporting information, Table S1. All *C. neoformans* strains were cultured in YPD (yeast extract-peptone-dextrose) medium unless indicated separately. L-DOPA or Niger seed medium for melanin production and agar-based Dulbecco's modified Eagle's (DME) medium for capsule production were all as described (Granger *et al.* 1985; Alspaugh *et al.* 1997; Bahn *et al.* 2004; Hicks *et al.* 2004).

Construction of the P_{CTR4}::*CAN2* promoter replacement strain: To replace the native *CAN2* promoter with the *CTR4* promoter, the *CAN2* promoter replacement cassette was generated as follows. The left flanking region [the *CAN2* promoter region spanning from −1192 to −376, relative to the ATG start codon (+1 to +3)] and the right flanking region

(*CAN2* gene, +1 to +1147 region) were PCR amplified with primer pairs B357/B358 and B359/B93, respectively. The underlined sequences of primers B358 and B359 in Table S1 overlap with those of the *NAT-CTR4* promoter insert of plasmid pNAT-CTR4-2 (kindly provided by John Perfect, Duke University). The *NAT-CTR4* promoter fragment was PCR-amplified with two primers B354 and B355. The *CAN2* promoter replacement cassette was generated by overlap PCR with two primers B357 and B93, gel extracted, precipitated onto 600-μg of gold microcarrier beads (0.6 μm, BioRad), and introduced into the serotype A *C. neoformans* strain H99 strain via biolistic transformation (Davidson *et al.* 2002). Stable transformants were selected on YPD medium containing nourseothricin (100 mg/liter). The P_{CTR4}::*CAN2* promoter replacement strains were screened by diagnostic PCR and Southern blot analysis using a *CAN2*-specific probe generated by PCR with primers B359 and B93.

Total RNA isolation: For total RNA isolation used in DNA microarray analyses, the WT H99 and P_{CTR4}::*CAN2* strains were cultured in 50 ml YPD medium at 30° for 24 hr, washed with sterile PBS buffer twice, and resuspended with sterile water. Then 1 ml of resuspended cells was innoculated into 100 ml of YNB medium (optical density at 600 nm is ~0.2) and incubated for 12 hr. For zero-time samples, 50 ml out of the 100-ml culture was used. Then 20 ml of the resuspended culture was inoculated into 200 ml of fresh YNB medium containing either 200 μM bathocuproinedisulfonic acid (BCS) for induction of *CAN2* or 25 μM copper sulfate ($CuSO_4$) for repression of *CAN2*, and further incubated for up to 36 hr at 30°. During incubation, 50 ml of the culture was sampled after 6, 12, 24, and 36 hr and used for total RNA isolation. As biological replicates for DNA microarray, three independent cultures for each strain and growth condition were prepared for total RNA isolation. Total RNAs were isolated by using TRizol reagent as previously described (Ko *et al.* 2009).

DNA microarray and data analysis: For an experimental set of total RNAs (Cy5 labeling), we used three independent total RNA samples that were isolated from each WT H99 and P_{CTR4}::*CAN2* strain grown for 12 hr in YNB containing either BCS or $CdSO_4$. For control total RNA (Cy3 labeling), all of the total RNAs prepared from WT and P_{CTR4}::*CAN2* strains grown in the conditions described above were pooled (pooled reference RNAs). For cDNA synthesis, Cy5/Cy3 labeling, prehybridization, hybridization, and slide washing, we followed the protocols described previously (Ko *et al.* 2009). For DNA microarray slides, we utilized *C. neoformans* serotype D (JEC21) 70-mer oligonucleotide microarray slides containing 7936 spots (Duke University). Three independent DNA microarrays with three independent biological replicates were performed.

The DNA microarray slides were scanned with a GenePix 4100A scanner (Axon Instrument) and the scanned images were analyzed with GenePix Pro (ver. 6.0) and gal file (http://genomeold.wustl.edu/activity/ma/cneoformans/array_spec.cgi). For array data analysis, we used the serotype A gene identification (ID) database that has been mapped to each corresponding 70-mer oligonucleotide sequence printed on the array slides as previously described (Ko *et al.* 2009). The JEC21 oligomer chip covers 6302 genes of the total 6980 genes in the H99 strain with an *e*-value $1e^{-6}$ (90% coverage) by blastn search. Each *S. cerevisiae* gene name or ID listed in Table S1, Table S2, Table S3, Table S4, and Table S5 was identified by blastp search with the serotype A gene sequence, (*e*-value cutoff: e^{-6}). For hierarchical and statistical analysis, data transported from GenePix software were analyzed with Acuity software by employing LOWESS normalization, reliable gene filtering (>95% filtering), hierarchical clustering, zero transformation, ANOVA analysis ($P < 0.05$), and Excel software (Microsoft).

Construction of the *cas3*Δ and *atf1*Δ mutant strains: The gene disruption cassettes for the *CAS3* and *ATF1* genes were constructed by double joint PCR with *NAT* split marker or overlap PCR by using primers listed in Table S1 as previously described (Davidson *et al.* 2002; Kim *et al.* 2009). For amplification of *NAT* marker, plasmid pNATSTM#220 for *ATF1* and pNATSTM#122 for *CAS3* were used as templates (Table S1). Purified gene disruption cassettes were introduced into the H99 strain by biolistic transformation. Each mutant was screened and confirmed by both diagnostic PCR and by Southern blot analysis.

Northern hybridization: Northern blot analysis was performed with 10 μg of total RNA from each strain that was used for DNA microarray analysis. Electrophoresis, probe preparation and radiolabeling, hybridization, and development were carried out by following the standard protocols previously described (Ausubel *et al.* 1994; Ko *et al.* 2009).

Growth and stress-response assay: For quantitative growth assays, the WT H99 and P_{CTR4}::*CAN2* (YSB734) strains were cultured overnight at 30° in liquid YPD medium, inoculated into YNB liquid medium containing 200 μM BCS and 25 μM $CuSO_4$, and further incubated at 30° for 6, 12, and 24 hr. After the indicated time of incubation, a portion of the cultures was sampled, serially diluted, spread onto duplicate YPD agar plates, and incubated at 30°. After 2 days, colony-forming units (CFUs) per each plate were determined. Stress and antifungal drug sensitivity tests were performed as previously described (Ko *et al.* 2009; Maeng *et al.* 2010).

Capsule and melanin assays: Qualitative visualization and quantitative measurement of capsule and melanin production was performed as described previously (Bahn *et al.* 2004). For additional quantitative measurement of capsule size, packed cell volume was also measured by using hematocrit capillary tubes. Briefly, cells grown on DME medium for 2 days were scraped, washed with PBS buffer to remove released polysaccharide, and fixed with 10% formalin. Cell concentration was determined by using hemocytometer and adjusted to 1×10^9 cells/ml with PBS buffer. Forty microliters of the cell suspension was loaded into microhematocrit capillary tubes (Hirschmann Labogeräte, no. 9100275), of which tips were sealed with clay and parafilm to prevent evaporation of medium during incubation. The capillary tubes were placed vertically overnight at room temperature to allow cell packing by gravity. The packed volume of cells was measured by ratio length of packed cell volume phase/length of total volume phase. Two or three independent experiments were performed in triplicate. Statistical difference in relative capsule size between strains was determined by Bonferroni's multiple comparison test by using Prism 4 software (GraphPad).

Microarray data accession number: The microarray data generated by this study was submitted to the Gene Expression Omnibus (GEO) (http://www.ncbi.nlm.nih.gov/geo/) with accession number GSE21192.

RESULTS

Construction of the P_{CTR4}::*CAN2* strain for artificially controlling of *CAN2* expression: To construct the *CAN2* promoter replacement strain, the 375-bp *CAN2* promoter region was replaced with the 2-kb fragment of the *CTR4* promoter and the *NAT* dominant selectable maker (Figure 1A). We verified the correct genomic organization of the P_{CTR4}::*CAN2* allele by Southern blot analysis with *Xba*1/*Xho*1- or *Hin*dIII-digested genomic DNAs (Figure 1B and data not shown). Four indepen-

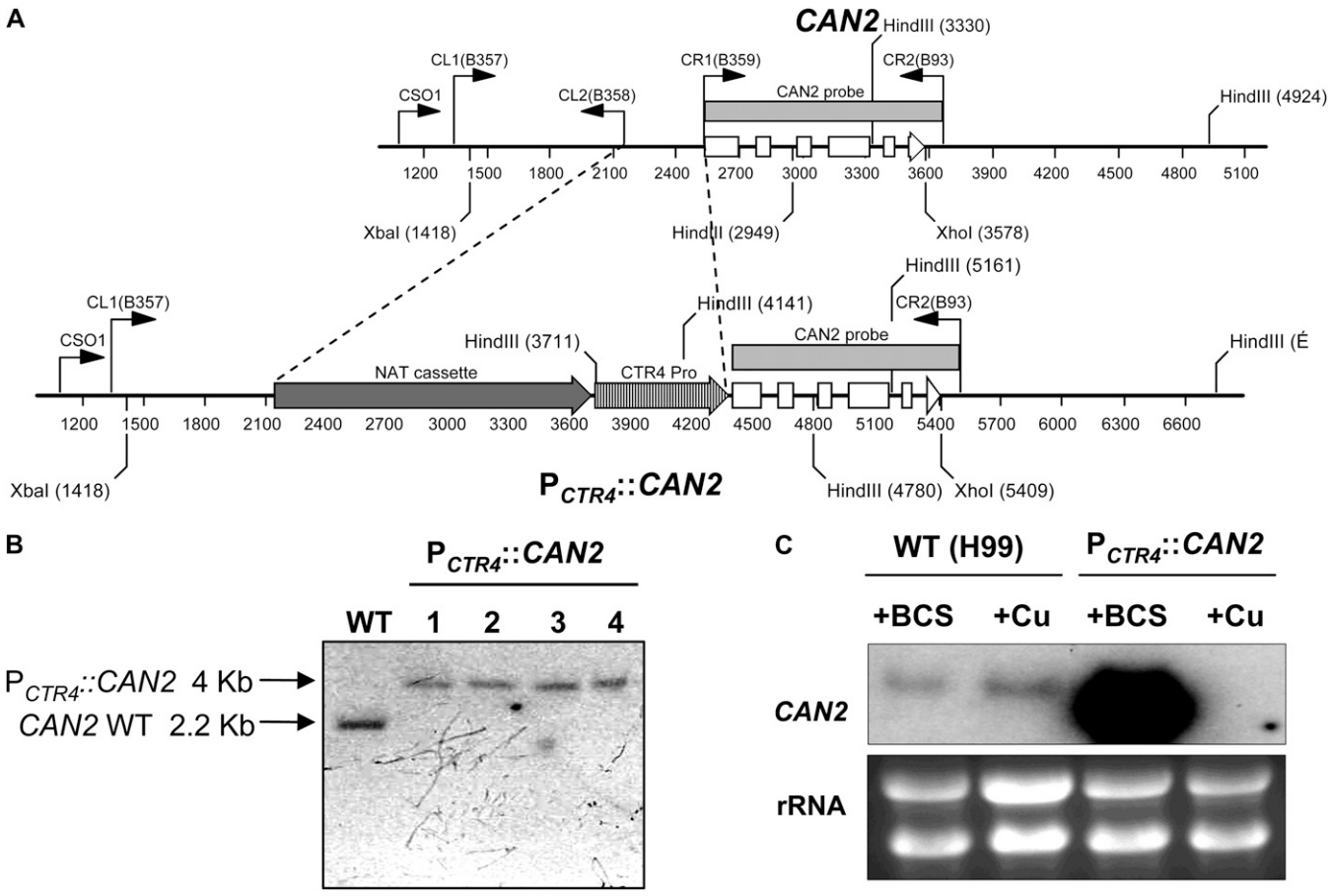

FIGURE 1.—Construction of the P_{CTR4}::*CAN2* promoter replacement strain. (A) The strategy for construction of the *CAN2* promoter replacement allele with the *CTR4* promoter. The first five exons of the *CAN2* gene are illustrated as open boxes and an arrow for exon 6 depicts the direction of transcription. Primers for overlap PCR and diagnostic PCR are indicated as bent arrows. The shaded arrow box illustrates a *NAT* selectable marker, which consists of *ACT1* promoter, *NAT* (nourseothricin acetyltransferase) gene, and *TRP1* terminator, and the shaded, striped arrow box illustrates the *CTR4* promoter as previously described (ORY *et al.* 2004). (B) Verification of the P_{CTR4}::*CAN2* strain by Southern hybridization. Each genomic DNA was digested with *Xba*I and *Xho*I and blotted membrane was probed with *CAN2*-specific probe that was PCR amplified with primers B359 and B93. WT indicates the H99 strain and lanes 1 to 4 indicate the independently isolated P_{CTR4}::*CAN2* strains (YSB733, YSB734, YSB735, and YSB736, respectively). (C) Northern hybridization of the controlled *CAN2* expression by the *CTR4* promoter. The WT H99 strain and the P_{CTR4}::*CAN2* strain (YSB734) were grown overnight at 30° in liquid YPD medium and subcultured into a fresh YNB liquid medium containing 200 μM BCS (+BCS) and 25 μM CuSO4 (+Cu). After a 12 hr-incubation, a portion of cultures was sampled and its total RNAs was isolated for Northern blot analysis as described in MATERIALS AND METHODS.

dent P_{CTR4}::*CAN2* strains were confirmed and employed for further analyses.

We further verified whether *CAN2* expression levels in the P_{CTR4}::*CAN2* strains are modulated by adding "BCS (a copper chelator) or CuSO4," which activates or represses the *CTR4* promoter, respectively. Northern blot analysis showed that *CAN2* expression levels in the P_{CTR4}::*CAN2* strains were strongly induced by addition of BCS and repressed by addition of $CuSO_4$ (Figure 1C), indicating that *CAN2* expression levels can be modulated by controlling copper levels in the growth media. *CAN2* expression levels in the P_{CTR4}::*CAN2* strains grown in the presence of BCS were even higher than native *CAN2* expression levels in the WT strain grown in the presence of BCS (Figure 1C), suggesting that the *CTR4* promoter is stronger than the *CAN2* promoter under copper-depleted conditions.

The P_{CTR4}::*CAN2* strain exhibited conditional growth defects in response to copper levels: We addressed whether the growth of P_{CTR4}::*CAN2* strains could be controlled under ambient air conditions by changing copper levels in the medium. The P_{CTR4}::*CAN2* strains did not show any growth defects in YNB medium containing BCS, which activates the *CTR4* promoter, whereas the strains exhibited severe growth defects in YNB medium containing $CuSO_4$, which represses the *CTR4* promoter (Figure 2A). A normal growth ability of the P_{CTR4}::*CAN2* strains was restored in the presence of high CO_2 concentrations (5%) (Figure 2A), further confirming that the growth defects observed in the P_{CTR4}::*CAN2* strains under the copper-depleted conditions were caused by reduced expression of *CAN2*. The growth defect of the P_{CTR4}::*CAN2* strains was also quantitatively measured

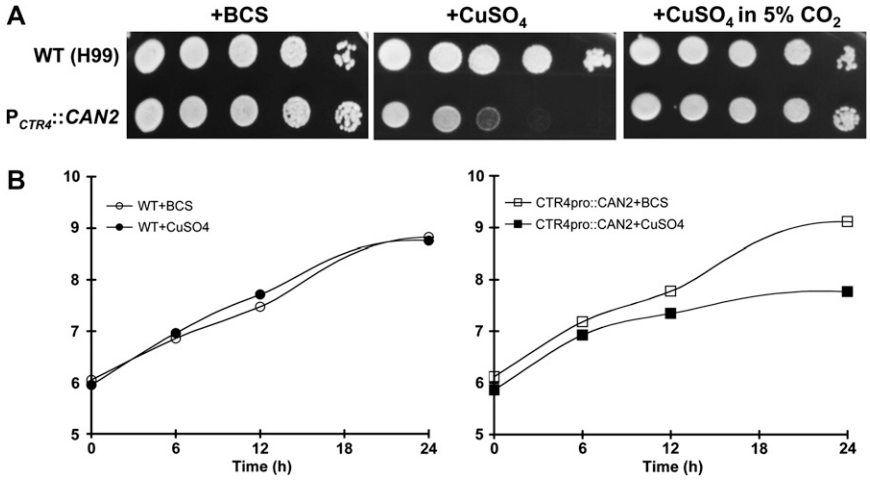

FIGURE 2.—Growth of the P_{CTR4}::*CAN2* strain is tightly controlled by copper levels in a CO_2-dependent manner. (A) The wild-type H99 and P_{CTR4}::*CAN2* (YSB734) strains were grown overnight at 30° in liquid YPD medium, 10-fold serially diluted (1–10^4 dilutions), and spotted (3 μl of dilution) on YNB agar containing 200 μM BCS and 25 μM $CuSO_4$. Cells were incubated at 30° for 24 hr under either normal air or high CO_2 conditions (5%) and photographed. (B) Quantitative growth assay of the P_{CTR4}::*CAN2* strain. The wild-type H99 and P_{CTR4}::*CAN2* (YSB734) strains were grown overnight at 30° in liquid YPD medium and inoculated into YNB liquid medium containing 200 μM BCS and 25 μM $CuSO_4$. Cells were incubated at 30° for 6, 12, and 24 hr, and a portion of cultures was sampled, serially diluted, and spread on YPD agar medium for viable cell count. Three independent experiments were performed and one representative graph was demonstrated. All three 12-hr total RNA samples were confirmed for differential *CAN2* regulation by Northern hybridization (data not shown) and used for subsequent DNA microarray analysis.

in liquid YNB medium containing either BCS or $CuSO_4$ at different time points. In agreement with results described above, the P_{CTR4}::*CAN2* strains also showed growth defects in the liquid YNB medium containing $CuSO_4$, but not BCS (Figure 2B). Taken together, our results demonstrate that *CAN2* expression is tightly controlled by the replaced *CTR4* promoter, which enables the precise control of *C. neoformans* growth under ambient air conditions, depending on copper levels in the culture medium.

Identification of Can2-dependent genes by comparative transcriptome analysis of the P_{CTR4}::*CAN2* strain and the wild-type *C. neoformans*: To identify CA-regulated genes, we performed genome-wide comparative transcriptome analysis of the WT and P_{CTR4}::*CAN2* strains grown in the presence of BCS or $CuSO_4$ by using DNA microarrays as described in MATERIALS AND METHODS.

First we compared genome-wide expression profiles of the P_{CTR4}::*CAN2* strains under copper-depleted conditions (+BCS), which showed normal growth patterns with induced *CAN2* expression, with those under copper-enriched conditions (+Cu), which showed retarded growth patterns with repressed *CAN2* expression. A total of 133 genes (120 genes with serotype A gene ID) exhibited significantly different expression levels (ANOVA, $P < 0.05$) (Figure 3A). Among these, 9 genes were differentially regulated in the WT strain between BCS and $CuSO_4$-containing media, indicating that these genes are copper-dependent genes. These genes include the *SOD1*, *LAC1*, and *CTR3* genes. The *CTR3* gene that encodes a copper transporter was most downregulated, mainly due to the increased copper concentrations in the growth medium. The *SOD1* and *LAC1* genes are also known to be induced by copper (CULOTTA *et al.* 1995; JIANG *et al.* 2009). Therefore, a total of 123 genes appeared to be *CAN2*-dependent genes. Among these, only 10 genes exhibited >1.5-fold induction or reduction when *CAN2* is repressed. As expected, the *CAN2* gene was the most highly repressed gene (Figure 3B), further verifying the quality of our microarray results. Upregulation of the *FUR1* gene, encoding uracil phosphoribosyltransferase, upon repression of the *CAN2* gene is notable. Previously we have hypothesized that the *can2* mutation inhibits cellular growth by affecting a variety of decarboxylating enzymes that use bicarbonate as a substrate and are required for biosynthesis of lipid, amino acids, and pyrimidines (BAHN *et al.* 2005). Therefore, it is conceivable that reduced pyrimidine biosynthesis by *CAN2* repression allows cells to induce the *FUR1* gene, which is one of the genes in the pyrimidine salvage pathway.

CAN2 expression levels induced by the *CTR4* promoter were higher than those by the *CAN2* native promoter in the presence of BCS (Figure 1C). Therefore, we compared transcriptome profiles of the WT and *CAN2*-promoter replacement strains in the presence of BCS. A greater number of genes (524 genes) were significantly and differentially regulated (ANOVA, $P < 0.05$) (Figure 4A). Among these, a total of 136 genes (128 genes with serotype A ID) showed >1.5-fold induction or reduction and only 10 genes showed more than twofold regulation (Figure 4B). Except the *CAN2* gene, only two genes, CNAG_04307.2 (uricase, named *URI1*) and CNAG_06917.2 (peroxiredoxin, named *PRX1*), have predicted functions based on sequence homology (Figure 4C). Regulation of the uricase gene appears to be related to CA and CO_2 metabolism. Uricase catalyzes the oxidation of uric acid to 5-hydroxyisourate, which can interact with H_2O_2 to produce allantoin and carbon dioxide.

On the basis of these array results, we further defined a true Can2-dependent gene based on the following criteria. First a Can2-dependent gene should be identi-

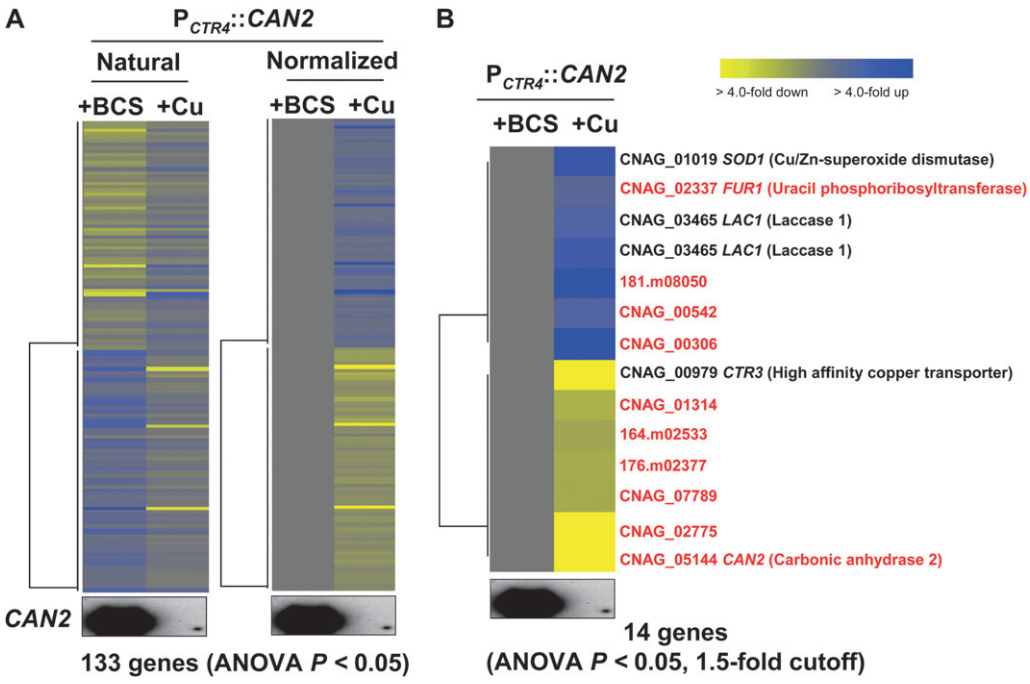

FIGURE 3.—Genes regulated by differential *CAN2* expression in the P$_{CTR4}$::*CAN2* strain. (A) The hierarchical clustering analysis of 133 genes, which exhibited significantly different expression patterns (ANOVA test, $P < 0.05$) by comparing the transcriptome of the P$_{CTR4}$::*CAN2* strain grown in YNB containing 200 μM BCS (+BCS, *CAN2* overexpression) or 25 μM $CuSO_4$ (+Cu, *CAN2* repression) after a 12-hr incubation. (B) The tree view of 14 genes, which exhibited >1.5-fold induction or repression among genes showing significantly different expression patterns (ANOVA test, $P < 0.05$). The fold change is illustrated by color (see color bar scale in B).

fied from both array data sets with statistical significance (ANOVA, $P < 0.05$). Second, the Can2-dependent gene should exhibit opposite expression patterns in each data set. Following these criteria, we have selected 17 Can2-dependent genes except *CAN2* itself (Table 1). These include *MEU1*, *GPB1*, *NAP1*, *FAS1*, *CFO2*, *CAS3*, and *ATF1*; a majority of these (9 of 17 genes) do not have orthologs in other fungi. The *FAS1* gene encodes fatty acid synthase and has been reported to be essential for survival of *C. neoformans* (CHAYAKULKEEREE *et al.* 2007). The *MEU1* gene encodes methylthioadenosine phosphorylase, which is the initial enzyme catalyzing the methionine salvage pathway (SUBHI *et al.* 2003). The *GPB1* gene encodes the Gβ-subunit in the pheromone response MAPK pathway and positively controls sexual differentiation of *C. neoformans* (WANG *et al.* 2000). These data further confirm that the CO_2-sensing carbonic anhydrase signaling pathway is closely connected to the fatty acid and amino acid biosynthetic pathways and sexual differentiation of *C. neoformans* as previously proposed (BAHN *et al.* 2005).

The role of Cas3 in capsule production of *C. neoformans*: *CAS3* is one of a few genes whose expression is positively regulated by *CAN2* overexpression in our array analysis (Table 1). Although it is homologous to Cap64, which is required for capsule production, Cas3 is not directly involved in capsule formation but instead is required for O-acetylation of the capsule in *C. neoformans* (MOYRAND *et al.* 2004). However it is still possible that Cas3 is indirectly involved in capsule production through regulation of other capsule genes as the authors speculated (MOYRAND *et al.* 2004). Here we tested the possibility that Cas3 might be involved in CO_2-mediated capsule induction since it has been previously reported that capsule production of *C. neoformans* is increased by high CO_2 concentrations (GRANGER *et al.* 1985; VARTIVARIAN *et al.* 1993).

To address this hypothesis, we generated two independent *cas3*Δ mutants and tested their ability to produce capsule in either ambient air or high CO_2 concentrations (Figure S1). Based on quantitative measurements of capsule production, the WT strain exhibited greatly enhanced capsule production in the presence of high CO_2 (5%) conditions (Figure 5A). In contrast, the *cac1*Δ mutant that is highly defective in capsule production under ambient air did not show any enhanced levels of capsule in response to high CO_2 concentrations (Figure 5A), indicating that CO_2-mediated capsule induction is required for activation of adenylyl cyclase, which has been proposed before (BAHN and MÜHLSCHLEGEL 2006). The two independent *cas3*Δ mutants exhibited WT levels of capsule under ambient air conditions (Figure 5A), as previously reported (MOYRAND *et al.* 2004). In response to high CO_2 concentration, the *cas3*Δ mutants also showed enhanced capsule production like the WT H99 strain (Figure 5A), indicating that Cas3 is not required for CO_2-mediated capsule induction.

We also tested whether overexpression of *CAN2* may enhance capsule production by growing the P$_{CTR4}$::*CAN2* strains in DME + BCS medium. We hypothesized that increased production of intracellular bicarbonate by *CAN2* overexpression might activate adenylyl cyclase, resulting in enhanced capsule induction. Unexpectedly, however, the P$_{CTR4}$::*CAN2* strains exhibited WT levels of capsule in DME + BCS medium

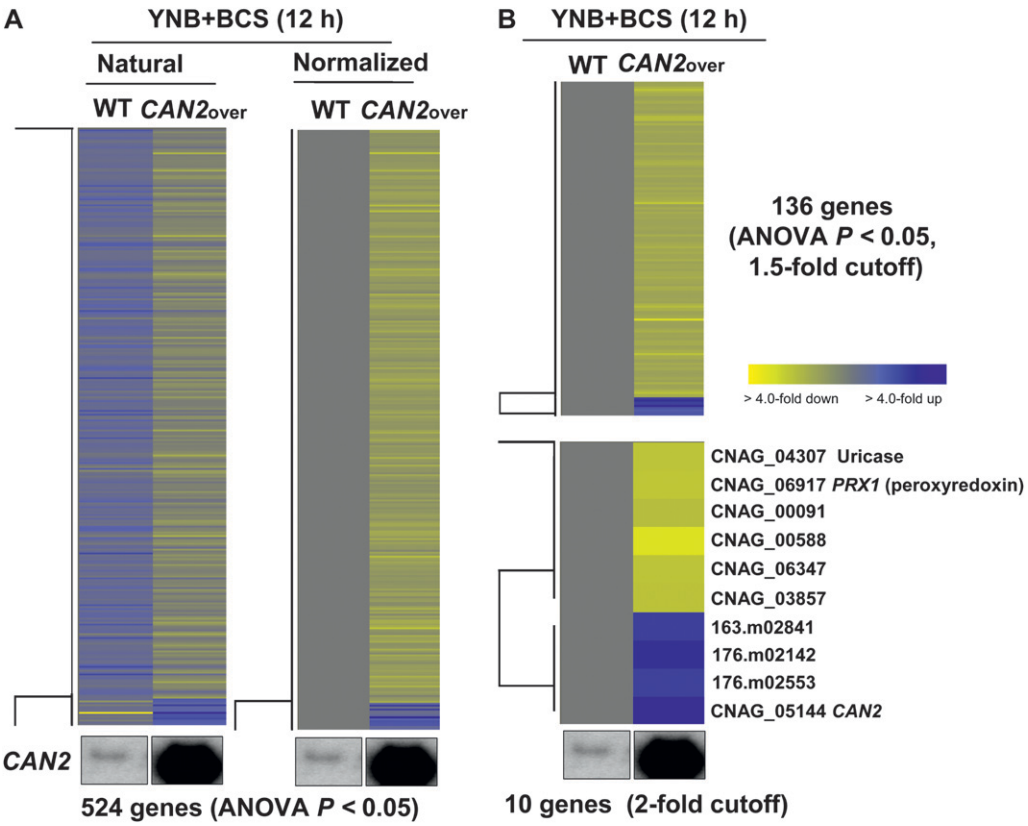

FIGURE 4.—Genes regulated by *CAN2* overexpression. (A) The hierarchical clustering analysis of 524 genes, which exhibited significantly different expression patterns (ANOVA test, $P < 0.05$) by comparing the transcriptomes of the wild-type H99 (WT) and P_{CTR4}::*CAN2* strains "*CAN2*over" grown in YNB containing 200 μM BCS after a 12-hr incubation. (B) The tree view of 136 and 10 genes, which exhibited >1.5-fold or twofold, respectively, induction or repression among genes showing significantly different expression patterns (ANOVA test, $P < 0.05$). The fold change is illustrated by color (see color bar scale in B).

under either ambient air or high CO_2 conditions (Figure 5B). In conclusion, *CAN2* overexpression does not enhance capsule induction in *C. neoformans*, although adenylyl cyclase is required for CO_2-mediated capsule induction.

ESR genes are regulated by Can2: A recent genome-wide transcriptome analysis of the stress-activated HOG pathway uncovered a number of ESR genes, whose expression is affected by osmotic shock, antifungal drug, or oxidative stress in *C. neoformans* (Ko *et al.* 2009). Interestingly, a majority of the Can2-dependent genes (11 of 17 genes) were found to be ESR genes of *C. neoformans* (Table 1). This finding suggests that *CAN2* overexpression can be sensed as stress because increased levels of bicarbonate and protons may change normal cellular physiological conditions. To test this hypothesis, we performed diverse stress sensitivity tests with the P_{CTR4}::*CAN2* strains grown on YNB + BCS medium (Figure 6). The P_{CTR4}::*CAN2* strains exhibited hypersensitivity to several stress-inducing agents, including H_2O_2, $CdSO_4$, and methylmethane sulfonate (MMS) compared to the WT strain. This indicates that *CAN2* overexpression render cells hypersensitive to oxidative and genotoxic stress. However, the P_{CTR4}::*CAN2* strains were as sensitive to hydroxyurea (HU), which is another genotoxic stress agent, as the WT strain.

The P_{CTR4}::*CAN2* strains exhibited extreme sensitivity to amphotericin B as well as azole drugs, such as fluconazole, ketoconazole, and itraconazole (Figure 6). These indicate that increased antifungal drug susceptibility of the P_{CTR4}::*CAN2* strains appears to be independent of the ergosterol biosynthesis because the phenotypes of the P_{CTR4}::*CAN2* strains were distinct from those of *hog1*Δ mutants that are defective in ergosterol biosynthesis (Figure 6). Instead, hypersensitivity of the P_{CTR4}::*CAN2* strain to antifungal drugs may result from its defective membrane integrity because the P_{CTR4}::*CAN2* strains exhibited increased sensitivity to SDS. Taken together, *CAN2* overexpression alters normal cellular physiology, which results in defective responses to diverse environmental stresses and antifungal drugs.

The role of the transcription factor Atf1 regulated by Can2: Among the Can2-dependent genes, the one encoding the transcription factor Atf1 was notable, although it does not belong to ESR genes (Table 1). Northern blot analysis confirmed that *ATF1* expression was slightly upregulated when *CAN2* is repressed, but slightly downregulated when *CAN2* is overexpressed (Figure S2), similar to the microarray results. Atf1 is a major transcription factor activated by the stress-activated Sty1 (a Hog1 MAPK homolog) MAPK in *Schizosaccharomyces pombe* (Shiozaki and Russell 1996; Wilkinson *et al.* 1996; Degols and Russell 1997). In *C. neoformans*, the thioredoxin system is controlled by Atf1, indicating that Atf1 is involved in oxidative stress response (Missall and Lodge 2005). However, the function of Atf1 in diverse stress responses and its relationship with the HOG pathway in *C. neoformans* still remains unknown.

TABLE 1

Can2-dependent genes in *C. neoformans*

SeroA ID (CNAG)	*C. ne* gene name	*S. ce* gene name	*S. po* gene name	Fold changes (log_2 scale) *CAN2* repressed	Fold changes (log_2 scale) *CAN2* overexressed	Function	Crypto-ESR
00054	None	None	None	0.308	−0.397	DUF1264 domain-containing protein	OxR-up OsR-dw
00165	None	*MEU1*	None	0.313	−0.613	Methylthioadenosine phosphorylase	
00906	None	None	None	0.365	−0.661	Nucleolar protein	
01262	*GPB1*	*STE4*	*Git5*	0.333	−0.482	G-protein beta subunit *GPB1*	OxR-dw
02091	None	*NAP1*	*NAP1*	0.343	−0.59	Nucleosome assembly protein	OxR-up
02099	*FAS1*	*FAS1*	*FAS1*	0.453	−0.67	Fatty acid synthase beta subunit	OxR-dw FxR-dw
02741	None	*OCT1*	None	0.399	−0.831	Mitochondrial intermediate peptidase	
02958	*CFO2*	None	None	0.549	−0.286	Ferroxidase	OsR-dw
03544	None	None	None	0.259	−0.52	Conserved hypothetical protein	OxR-dw
03644	*CAS3*	None	None	−0.461	0.344	Cap64 homologs	
04090	*ATF1*	None	*ATF1*	0.347	−0.483	Activating transcription factor 2	
04837	None	None	None	0.422	−0.461	Conserved hypothetical protein	
05976	None	*NOP58*	None	−0.338	0.262	SnoRNA binding domain containing protein	OxR-dw OsR-up
06356	None	None	None	0.189	−0.447	Mitochondrial protein	OxR-dw
06668	None	*AIM38*	None	0.538	−0.284	Mitochondrial protein	FxR-dw
06968	None	None	None	0.154	−0.493	Hypothetical protein	OxR-dw
07465	None	None	None	−0.449	0.72	Conserved hypothetical protein	OxR-dw

C. ne, Cryptococcus neoformans; *S. ce, Saccharomyces cerevisiae*; *S. po, Schizosaccharomyces pombe*; ESR, environmental stress regulated; OxR-up/dw, up- or down-regulated by oxidative stress; OsR-up/dw, up- or down-regulated by osmotic stress; FxR-up/dw, up- or down-regulated by fludioxonil.

Therefore, we independently constructed the *atf1*Δ mutant strain in the WT H99 strain that retains full virulence (Figure S3) and tested various stress sensitivities and virulence factor production compared with the mutants of the stress-activated HOG pathway and other stress-related signaling pathways such as the Ras and cAMP pathways. As control strains, we used the *atf1*Δ mutant (here designated as *atf1*ΔE), which was previously constructed in the H99-Eunuch strain background (H99E) (Missall and Lodge 2005).

The two independently generated *atf1*Δ mutants exhibited the expected hypersensitivity to *tert*-butyl hydroperoxide (*t*BOOH) similar to the *atf*ΔE mutant (Figure 7) as previously reported (Missall and Lodge 2005). The *atf1*Δ mutants also exhibited hypersensitivity to H_2O_2, but hyperresistance to diamide (Figure 7). Furthermore, the *atf1*Δ mutant showed increased sensitivity to high temperature (40°) and the toxin methylglyoxal (Figure 7). These stress-response phenotypes of the *atf1*Δ mutant are similar to those of the *hog1*Δ mutant. In contrast, the *atf1*Δ mutant did not show any increased sensitivity to osmotic shock, cell wall/membrane-destabilizing agents such as SDS, and genotoxic agents, such as hydroxyurea and methylmethane sulfonate (Figure 7 and Figure S4). As previously described (Ko *et al.* 2009), the *hog1*Δ and *ssk1*Δ mutants were more sensitive to osmotic shock under carbon-starvation conditions and the presence of hydroxyurea. Furthermore, the *atf1*Δ mutant exhibited rather unique antifungal drug resistance patterns, which were also distinguished from those of the *hog1*Δ, *ras1*Δ, and *cac1*Δ mutants (Figure 7). As previously reported, the *hog1*Δ mutant exhibited hypersensitivity to amphotericin B, but increased resistance to fluconazole and fludioxonil (Figure 7). However, the *atf1*Δ mutant exhibited increased resistance to both amphotericin B and fluconazole, but showed slightly enhanced sensitivity to fludioxonil (Figure 7). Notably, the *atf1*Δ mutant was much more sensitive to flucytosine treatment than the WT strain. Similarly, the *ras1*Δ mutant also exhibited hypersensitivity to flucytosine. In contrast, the *hog1*Δ, but not *cac1*Δ, mutant exhibited only slightly increased sensitivity to flucytosine (Figure 7). The stress and antifungal drug response phenotypes of the *atf1*ΔE mutant in the H99E background were generally identical to those of the *atf1*Δ mutants in the WT H99 background, although we have found several phenotypic differences between H99 and H99E strains (Figure 7). Since the H99E strain was more thermosensitive than the H99 strain, thermosensitivity of the *atf1*ΔE strain was not observed (Figure 7).

The *atf1*Δ mutant exhibited increased melanin and capsule production (Figure 8), which is similar to the *hog1*Δ mutant. In capsule production, both *atf1*Δ and *atf1*ΔE mutants exhibited higher levels of capsule than the H99 and H99E strains, respectively (Figure 8A). Similarly, melanin production was more enhanced in

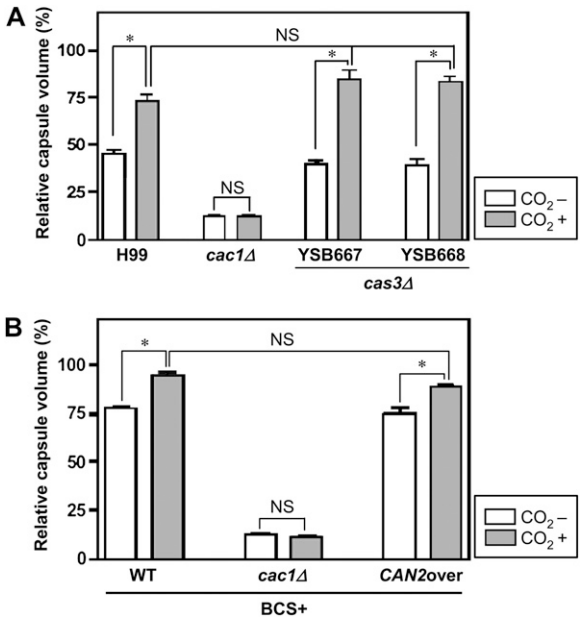

FIGURE 5.—The role of Cas3 and Can2 in CO_2-mediated capsule induction. Capsule synthesis levels of the following *C. neoformans* strains were quantitatively measured by using hematocrit as described in MATERIALS AND METHODS. The *Y*-axis indicates the relative capsule volume, which is percent ratio of length of packed cell volume phase *vs.* length of total loading volume phase. (A) *C. neoformans* strains [the wild-type H99 and *cac1*Δ (YSB42) and *cas3*Δ (YSB667 and YSB668) mutant strains] were grown in DME medium under either ambient air ($-CO_2$) or high CO_2 (5%, $+CO_2$) conditions for capsule induction. (B) *C. neoformans* strains [the wild-type H99 and *cac1*Δ (YSB42) and P_{CTR4}::*CAN2* (YSB734) mutant strains] were grown in DME medium containing 200 μM BCS under either ambient air ($-CO_2$) or high CO_2 (5%, $+CO_2$) conditions for capsule induction. Three independent experiments with triplicates were performed. Statistical analysis was performed by using Bonferroni multiple comparison test. $^*P < 0.001$ and NS, not significant ($P > 0.05$).

both *atf1*Δ and *aft1*ΔE mutants than the H99 and H99E strains, respectively (Figure 8B). Interestingly, the H99E strain was found to be highly defective in melanin production, which is similar to the *cac1*Δ mutant, compared to the H99 strain (Figure 8B). In both Nigher seed and L-DOPA media, the *atf1*Δ mutant exhibited increased melanin production (Figure 8B). Taken together, Atf1 appears to play important roles in response to environmental stress and antifungal drug treatment and production of melanin and capsule in a manner that is shared with and distinct from the HOG pathway in *C. neoformans*.

DISCUSSION

In this study, we aimed to elucidate the genes regulated by CA, which is essential for growth and differentiation of *C. neoformans*, on a genome-wide scale. To achieve this goal, we constructed the conditional *CAN2* expression mutant in which the native *CAN2* promoter is replaced with the *CTR4* promoter, which is controlled by the copper levels in the growth medium (ORY *et al.* 2004). The P_{CTR4}::*CAN2* strain exhibited growth defects when *CAN2* expression is repressed by addition of $CuSO_4$, but grew normally when the *CAN2* gene is overexpressed by addition of BCS. Expectedly, the growth defect was restored to normal by addition of high CO_2. As an additional benefit from this study, we could monitor *CAN2* overexpression phenotypes in media containing BCS because *CAN2* expression levels induced by the *CTR4* promoter were much higher than the native *CAN2* expression levels.

Through the comparative transcriptome analysis by DNA microarray with the P_{CTR4}::*CAN2* strain, we found several Can2-dependent genes in *C. neoformans*, which have not been reported before. To the best of our knowledge, this is the first genome-wide transcriptome analysis to discover the target genes directly or indirectly regulated by carbonic anhydrase in the CO_2-sensing and metabolic pathway. The majority of Can2-dependent genes appeared to be uniquely found in *C. neoformans*. However, the list of Can2-dependent genes that have predicted functions based on sequence homology, including *FUR1*, *URI1*, *PRX1*, *FAS1*, *GPB1*, *CAS3*, *CFO1*, *ATF1*, *MEU1*, *NAP1*, *OCT1*, *NOP58*, and *AIM38*, provided insight into the downstream signaling network modulated by CO_2 and CA in *C. neoformans*.

The *FAS1* (fatty acid synthase 1) gene was upregulated when *CAN2* is repressed, but downregulated when *CAN2* is overexpressed. This result may explain how fatty acid biosynthesis is regulated by CA. Previously we have shown that the growth defect of the *can2*Δ mutant can be partially restored to normal by exogenous addition of fatty acid, such as palmitate and myristate, indicating the role of Can2 in fatty acid biosythesis (BAHN *et al.* 2005). Therefore expression of the *FAS1* gene may be controlled as a compensatory mechanism for different CA activity and intracellular bicarbonate levels. Both Fas1 and Fas2 are known to be required for fatty acid biosynthesis and essential for growth of *C. neoformans* (CHAYAKULKEEREE *et al.* 2007).

Differential expression of *GPB1*, a Gβ-subunit of the pheromone-responsive Cpk1 MAPK pathway, also helps us to understand the role of Can2 in sexual differentiation of *C. neoformans*. Can2 is involved in both initial and terminal stages of sexual cycles of *C. neoformans* in negative and positive manners, respectively (BAHN *et al.* 2005). Our array data showing that basal expression levels of *GPB1* is induced when *CAN2* is repressed indicate that the Gpb1-mediated Cpk1 MAPK pathway can be controlled by Can2.

In *C. neoformans*, high CO_2 enhances capsule production (GRANGER *et al.* 1985; VARTIVARIAN *et al.* 1993). Originally we hypothesized that Can2-mediated *CAS3* induction may be responsible for enhancement of capsule production by high CO_2 concentration. Cas3 has been identified as one of a seven-member family of

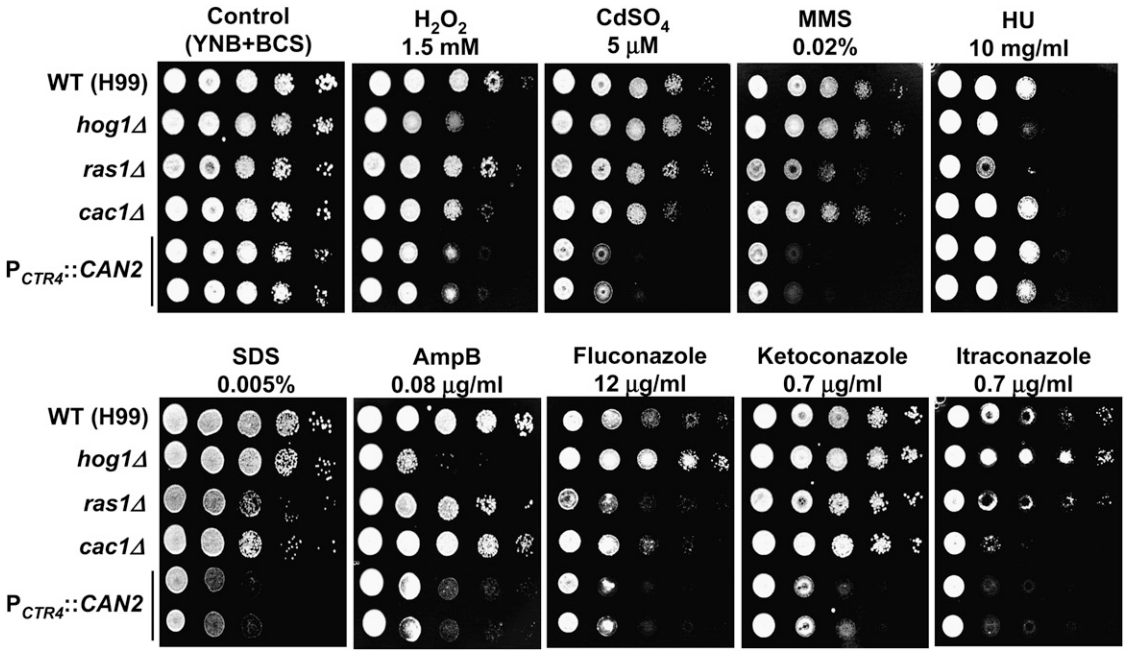

Figure 6.—The effect of *CAN2* overexpression in stress response. Each *C. neoformans* strain [the wild-type H99 and *ras1*Δ (YSB53), *cac1*Δ (YSB42), *hog1*Δ (YSB64), and P_{CTR4}::*CAN2* (YSB733 and YSB734) mutant strains] was grown overnight at 30° in liquid YPD medium, washed, 10-fold serially diluted (1–10^4 dilutions), and spotted (3 μl of dilution) on YNB agar medium containing 200 μM BCS and the indicated concentrations of hydrogen peroxide (H_2O_2), $CdSO_4$, methylmethane sulfonate (MMS), hydroxyurea (HU), SDS, amphotericin B (AmpB), fluconazole, ketoconazole, and itraconazole. Cells were incubated at 30° for 72 hr and photographed.

capsular structure designer proteins, although it is not directly involved in capsule formation but instead required for O-acetylation of the capsule in *C. neoformans* (Moyrand *et al.* 2004). Our data showed that Cas3 is not required for CO_2-mediated capsule induction. Mogensen and co-workers demonstrated that bicarbonate directly activates Cac1 adenylyl cyclase *in vitro*, which is the key component of the cAMP-signaling pathway, which plays a major role in capsule biosynthesis (Mogensen *et al.* 2006). Supporting this, we also found that CO_2-mediated capsule induction requires functional adenylyl cyclase *in vivo*. However, we have found that *CAN2* overexpression did not enhance capsule production in either ambient air or high CO_2 conditions. Therefore, it still remains elusive whether increased bicarbonate or activated Can2 directly activates adenylyl cyclase for capsule induction *in vivo*. It is also possible that unnatural *CAN2* overexpression by the *CTR4* promoter may affect other factors that counteract normal capsule induction.

One of the interesting findings of our array analysis is that a majority of Can2-dependent genes were ESR genes, whose expression is differentially regulated in response to environmental stresses, such as osmotic shock and oxidative stresses (Ko *et al.* 2009). The reason for regulation of the ESR genes by the *CAN2* gene is not clear. Differential expression of the *CAN2* gene will change intracellular levels of bicarbonate and proton, which affect intracellular pH and osmotic balance. xThese intracellular physiological changes can be sensed as stress, which may trigger cells to induce or repress ESR genes to counterbalance the stress. Supporting this, the *CAN2* overexpression strain was hypersensitive to oxidative stress (H_2O_2) and genotoxic stress (MMS).

Related to this finding, the transcription factor Atf1 was found to be differentially regulated by Can2. Atf1 is orthologous to *S. pombe* Atf1, which is a key downstream transcription factor of the stress-activated Sty1 MAPK (Shiozaki and Russell 1996; Wilkinson *et al.* 1996; Degols and Russell 1997). Although Missall and Lodge previously reported that Atf1 is involved in regulation of the thioredoxin system during oxidative stress response, here we further characterized the role of Atf1 in diverse stress response by using independently constructed *atf1*Δ mutants in the WT H99 strain background. The *atf1*Δ mutants that we generated generally exhibited identical phenotypes compared to the *atf1*ΔE mutants that Missall and Lodge generated in the H99E strain background. Minor phenotypic differences appear to result from the strain background difference. At this point, it is not clear whether Atf1 is the transcription factor working downstream of the HOG pathway. The *atf1*Δ mutant shared some of stress-response phenotypes with the *hog1*Δ mutant and yet exhibited phenotypes distinct from those of the *hog1*Δ mutant, including genotoxic stress and membrane-destabilizing response and antifungal drug resistance. It is possible that Atf1 may be responsible for a subset of HOG-dependent phenotypes. Whether Atf1

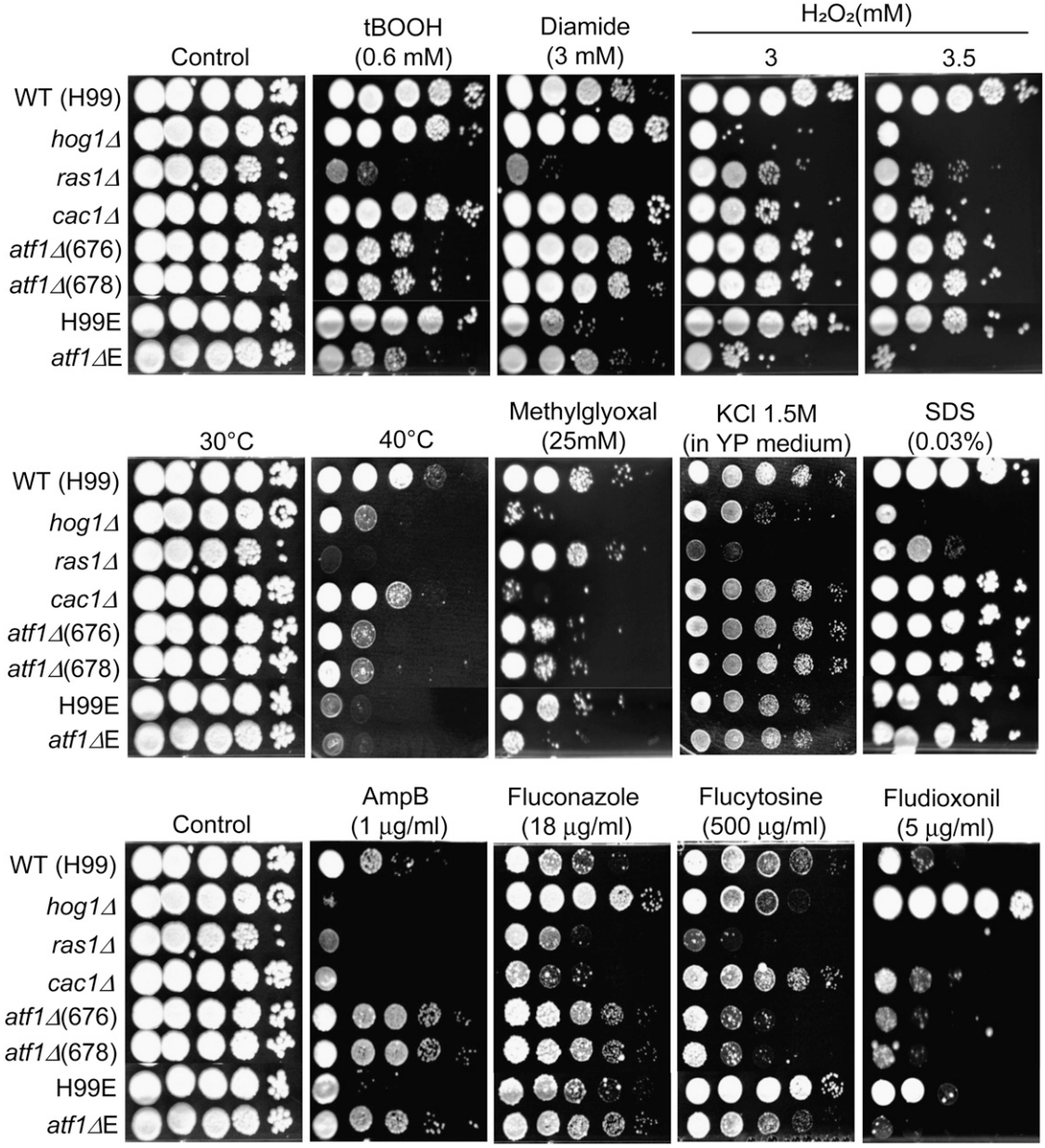

FIGURE 7.—The role of Atf1 in stress response and resistance to antifungal drugs. Each *C. neoformans* strain [the wild-type H99 and H99-Eunuch strains and *ras1*Δ (YSB53), *cac1*Δ (YSB42), *hog1*Δ (YSB64), *atf1*Δ (YSB676 and YSB678), and *atf1*ΔE (BE7-151) mutant strains] was grown overnight at 30° in liquid YPD medium, 10-fold serially diluted (1–10^4 dilutions), and spotted (3 μl of dilution) on YPD agar containing the indicated concentrations of hydrogen peroxide (H_2O_2), diamide, *tert*-butyl hydroperoxide (*t*BOOH), methylglyoxal, KCl, SDS, amphotericin B, fluconazole, flucytosine, and fludioxonil. Cells were incubated at 30° for 72 hr and photographed. For thermotolerance test, cells spotted on YPD medium were incubated at 40° for 4 days and photographed.

is a direct downstream effector for the Hog1 MAPK needs to be further addressed in future study.

Recently, Sheth and co-workers monitored global transcriptional response of *C. albicans* under 5.5% CO_2, which mimics host physiological conditions. Interestingly, among the 14 genes whose expressions are significantly changed by high CO_2, three of them (*HSP12*, *AAH1*, and *OPT1*) are known to be regulated by the HOG pathway (SHETH *et al.* 2008), indicating that CO_2 sensing and metabolism could also be related to the stress-response signaling pathway in *C. albicans*. Particularly, transcript abundance of *HSP12*, which encodes a small heat-shock protein involved in protein folding under stress conditions, are lowered by 5.5% CO_2 in an adenylyl cyclase/cAMP-dependent manner, suggesting that *C. albicans* considers ambient air having 0.036% CO_2 as stress. Supporting this finding, our recent transcriptome analysis of the cAMP-signaling pathway in *C. neoformans* demonstrated that two *HSP12* orthologous genes, *HSP12* and *HSP122*, are both

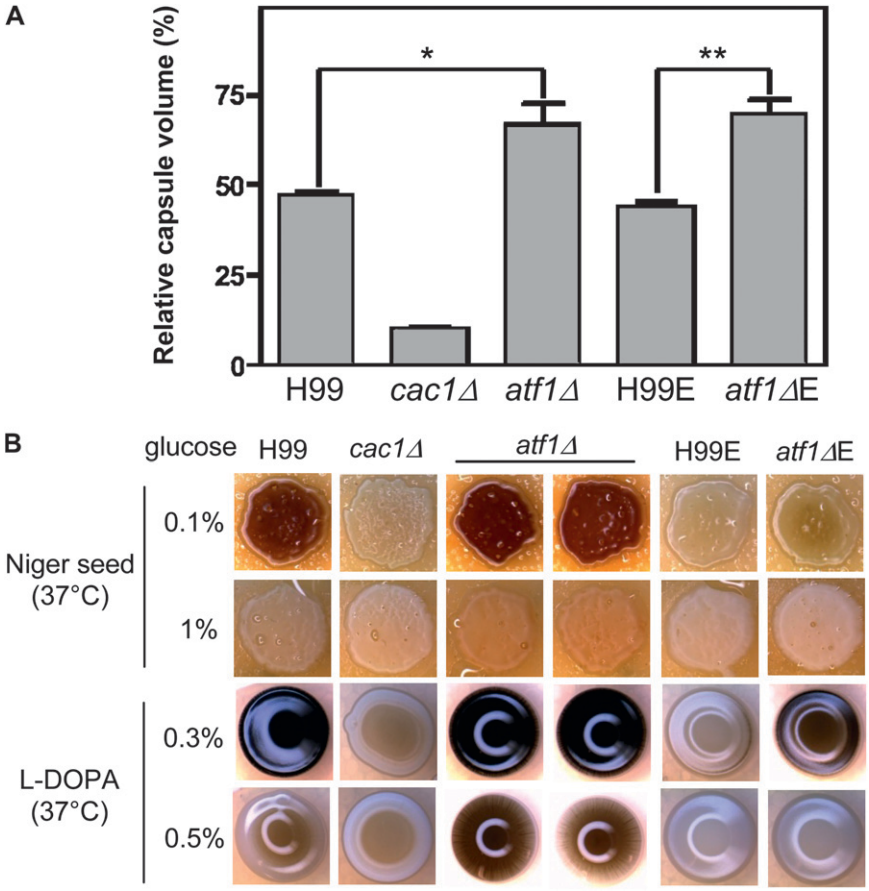

FIGURE 8.—The role of Atf1 in caspule and melanin production. (A) Capsule synthesis levels of *C. neoformans* strains [the wild-type H99 and H99-Eunuch strains and *cac1*Δ (YSB42), *atf1*Δ (YSB676), and *atf1*ΔE (BE7-151) mutant strains] were quantitatively measured by using hematocrit as described in MATERIALS AND METHODS and Figure 5A. Two independent experiments with triplicates were performed. Statistical analysis was performed by using Bonferroni multiple comparison test. $*P < 0.01$ and $**P < 0.001$, respectively. (B) For melanin production, the wild-type H99 and H99-Eunuch strains and *cac1*Δ (YSB42), *atf1*Δ (YSB676 and YSB678), and *atf1*ΔE (BE7-151) mutant strains were grown overnight (~16 hr) in YPD medium, spotted on solid Niger seed containing either 0.1 or 1.0% glucose or L-DOPA medium containing 0.3 or 0.5% glucose, incubated at 37° for 2 days, and photographed after 2 days.

regulated by cAMP and HOG pathways in the pathogen (MAENG *et al.* 2010).

The last notable finding of this study is a potential of Can2 and Atf1 as targets for combination antifungal therapy along with commercially known antifungal drugs. First, the *CAN2* overexpression strains were extremely sensitive to amphotericin B (AmpB) and azole drugs. Therefore, a molecule(s) that is able to induce activity of Can2 or expression of *CAN2* could be used for treatment of cryptococcosis along with AmpB and azole drugs. The synergistic mechanism between *CAN2* overexpression and AmpB or azole drugs is not clear at this point. It is possible that decreased *FAS1* expression in the *CAN2* overexpression strain may affect cell membrane integrity, which results in increased sensitivity to AmpB, which destroys membrane integrity or increased intracellular uptake of the antifungal drugs. Another benefit for the Can2-activating molecule could be decreased stress sensitivity of *C. neoformans*, which may result in rapid clearance during host infection. Second, the *atf1*Δ mutant was much more sensitive to flucytosine than the wild-type strain. Interestingly, the *ras1*Δ mutant was also found to be hypersensitive to flucytosine. These data indicate that an inhibitor of Atf1 or Ras1 in combination with flucytosine could be effective for treatment of cryptococcosis. The reason for this synergism is not understood at this point.

In conclusion, our CA-transcriptome analysis not only discovered a number of Can2-dependent genes in *C. neoformans*, but also made the finding that perturbed CO_2/bicarbonate homeostasis may cause impaired cellular response to diverse environmental stresses. Therefore, modulation of the signaling network of the CA/CO_2-sensing pathway may provide a novel therapeutic method for treatment of pathogenic fungi.

This work was supported by the Pioneer Research Center Program through the National Research Foundation of Korea, funded by the Ministry of Education, Science and Technology (no. 2009-0081512), the National Research Foundation of Korea grant, funded by the Korean government (MEST) (2009-0063344), and Yonsei University Research Fund of 2008 (2008-7-0285) (to Y.S.B). This work was also supported in part by RO1 grant AI50438 and R21 grant AI70230 from the National Institutes of Health/National Institute of Allergy and Infectious Diseases (to J.H.).

LITERATURE CITED

ALSPAUGH, J. A., J. R. PERFECT and J. HEITMAN, 1997 *Cryptococcus neoformans* mating and virulence are regulated by the G-protein α subunit GPA1 and cAMP. Genes Dev. **11:** 3206–3217.

AMOROSO, G., L. MORELL-AVRAHOV, D. MULLER, K. KLUG and D. SULTEMEYER, 2005 The gene *NCE103* (*YNL036w*) from *Saccharomyces cerevisiae* encodes a functional carbonic anhydrase and its transcription is regulated by the concentration of inorganic carbon in the medium. Mol. Microbiol. **56:** 549–558.

AUSUBEL, F. M., R. BRENT, R. E. KINGSTON, D. D. MOORE, J. G. SEIDMAN *et al.*, 1994 *Current Protocols in Molecular Biology*. Greene Publishing Associates and John Wiley & Sons, New York, NY

Bahn, Y. S., G. M. Cox, J. R. Perfect and J. Heitman, 2005 Carbonic anhydrase and CO_2 sensing during *Cryptococcus neoformans* growth, differentiation, and virulence. Curr. Biol. **15:** 2013–2020.

Bahn, Y. S., and F. A. Mühlschlegel, 2006 CO_2 sensing in fungi and beyond. Curr. Opin. Microbiol. **9:** 572–578.

Bahn, Y. S., J. K. Hicks, S. S. Giles, G. M. Cox and J. Heitman, 2004 Adenylyl cyclase-associated protein Aca1 regulates virulence and differentiation of *Cryptococcus neoformans* via the cyclic AMP-protein kinase A cascade. Eukaryot. Cell **3:** 1476–1491.

Chayakulkeeree, M., T. H. Rude, D. L. Toffaletti and J. R. Perfect, 2007 Fatty acid synthesis is essential for survival of *Cryptococcus neoformans* and a potential fungicidal target. Antimicrob. Agents Chemother. **51:** 3537–3545.

Clark, D., R. S. Rowlett, J. R. Coleman and D. F. Klessig, 2004 Complementation of the yeast deletion mutant Δ*NCE103* by members of the β class of carbonic anhydrases is dependent on carbonic anhydrase activity rather than on antioxidant activity. Biochem. J. **379:** 609–615.

Culotta, V. C., H. D. Joh, S. J. Lin, K. H. Slekar and J. Strain, 1995 A physiological role for *Saccharomyces cerevisiae* copper/zinc superoxide dismutase in copper buffering. J. Biol. Chem. **270:** 29991–29997.

Davidson, R. C., J. R. Blankenship, P. R. Kraus, M. de Jesus Berrios, C. M. Hull *et al.*, 2002 A PCR-based strategy to generate integrative targeting alleles with large regions of homology. Microbiology **148:** 2607–2615.

Degols, G., and P. Russell, 1997 Discrete roles of the Spc1 kinase and the Atf1 transcription factor in the UV response of *Schizosaccharomyces pombe*. Mol. Cell. Biol. **17:** 3356–3363.

Gotz, R., A. Gnann and F. K. Zimmermann, 1999 Deletion of the carbonic anhydrase-like gene *NCE103* of the yeast *Saccharomyces cerevisiae* causes an oxygen-sensitive growth defect. Yeast **15:** 855–864.

Granger, D. L., J. R. Perfect and D. T. Durack, 1985 Virulence of *Cryptococcus neoformans*. Regulation of capsule synthesis by carbon dioxide. J. Clin. Invest. **76:** 508–516.

Henry, R. P., 1996 Multiple roles of carbonic anhydrase in cellular transport and metabolism. Annu. Rev. Physiol. **58:** 523–538.

Hicks, J. K., C. A. D'Souza, G. M. Cox and J. Heitman, 2004 Cyclic AMP-dependent protein kinase catalytic subunits have divergent roles in virulence factor production in two varieties of the fungal pathogen *Cryptococcus neoformans*. Eukaryot. Cell **3:** 14–26.

Jiang, N., N. Sun, D. Xiao, J. Pan, Y. Wang *et al.*, 2009 A copper-responsive factor gene CUF1 is required for copper induction of laccase in *Cryptococcus neoformans*. FEMS Microbiol. Lett. **296:** 84–90.

Kim, M. S., S. Y. Kim, J. K. Yun, Y. W. Lee and Y. S. Bahn, 2009 An efficient gene disruption method in *Cryptococcus neoformans* by double-joint PCR with *NAT*-split markers. Biochem. Biophys. Res. Commun. **390:** 983–988.

Klengel, T., W. J. Liang, J. Chaloupka, C. Ruoff, K. Schroppel *et al.*, 2005 Fungal adenylyl cyclase integrates CO_2 sensing with cAMP signaling and virulence. Curr. Biol. **15:** 2021–2026.

Ko, Y. J., Y. M. Yu, G. B. Kim, G. W. Lee, P. J. Maeng *et al.*, 2009 Remodeling of global transcription patterns of *Cryptococcus neoformans* genes mediated by the stress-activated HOG signaling pathways. Eukaryot Cell **8:** 1197–1217.

Maeng, S., Y. J. Ko, G. B. Kim, K. W. Jung, A. Floyd *et al.*, 2010 Comparative transcriptome analysis reveals novel roles of the Ras and cyclic AMP signaling pathways in environmental stress response and antifungal drug sensitivity in *Cryptococcus neoformans*. Eukaryot. Cell **9:** 360–378.

Missall, T. A., and J. K. Lodge, 2005 Function of the thioredoxin proteins in *Cryptococcus neoformans* during stress or virulence and regulation by putative transcriptional modulators. Mol. Microbiol. **57:** 847–858.

Mock, R. C., J. H. Pollack and T. Hashimoto, 1990 Carbon dioxide induces endotrophic germ tube formation in *Candida albicans*. Can. J. Microbiol. **36:** 249–253.

Mogensen, E. G., G. Janbon, J. Chaloupka, C. Steegborn, M. S. Fu *et al.*, 2006 *Cryptococcus neoformans* senses CO_2 through the carbonic anhydrase Can2 and the adenylyl cyclase Cac1. Eukaryot. Cell **5:** 103–111.

Moyrand, F., Y. C. Chang, U. Himmelreich, K. J. Kwon-Chung and G. Janbon, 2004 Cas3p belongs to a seven-member family of capsule structure designer proteins. Eukaryot. Cell **3:** 1513–1524.

Ory, J. J., C. L. Griffith and T. L. Doering, 2004 An efficiently regulated promoter system for *Cryptococcus neoformans* utilizing the *CTR4* promoter. Yeast **21:** 919–926.

Parkkila, S., A. K. Parkkila, H. Rajaniemi, G. N. Shah, J. H. Grubb *et al.*, 2001 Expression of membrane-associated carbonic anhydrase XIV on neurons and axons in mouse and human brain. Proc. Natl. Acad. Sci. USA **98:** 1918–1923.

Schlicker, C., R. A. Hall, D. Vullo, S. Middelhaufe, M. Gertz *et al.*, 2009 Structure and inhibition of the CO_2-sensing carbonic anhydrase Can2 from the pathogenic fungus *Cryptococcus neoformans*. J. Mol. Biol. **385:** 1207–1220.

Sheth, C. C., E. G. Mogensen, M. S. Fu, I. C. Blomfield and F. A. Mühlschlegel, 2008 *Candida albicans HSP12* is co-regulated by physiological CO_2 and pH. Fungal Genet. Biol. **45:** 1075–1080.

Shiozaki, K., and P. Russell, 1996 Conjugation, meiosis, and the osmotic stress response are regulated by Spc1 kinase through Atf1 transcription factor in fission yeast. Genes Dev. **10:** 2276–2288.

Sims, W., 1986 Effect of carbon dioxide on the growth and form of *Candida albicans*. J. Med. Microbiol. **22:** 203–208.

Subhi, A. L., P. Diegelman, C. W. Porter, B. Tang, Z. J. Lu *et al.*, 2003 Methylthioadenosine phosphorylase regulates ornithine decarboxylase by production of downstream metabolites. J. Biol. Chem. **278:** 49868–49873.

Tripp, B. C., K. Smith and J. G. Ferry, 2001 Carbonic anhydrase: new insights for an ancient enzyme. J. Biol. Chem. **276:** 48615–48618.

Vartivarian, S. E., E. J. Anaissie, R. E. Cowart, H. A. Sprigg, M. J. Tingler *et al.*, 1993 Regulation of cryptococcal capsular polysaccharide by iron. J. Infect. Dis. **167:** 186–190.

Wang, L., P. Tornquist and A. Bill, 1997 Glucose metabolism in pig outer retina in light and darkness. Acta Physiol. Scand. **160:** 75–81.

Wang, P., J. R. Perfect and J. Heitman, 2000 The G-protein β subunit GPB1 is required for mating and haploid fruiting in *Cryptococcus neoformans*. Mol. Cell. Biol. **20:** 352–362.

Watson, P. H., S. K. Chia, C. C. Wykoff, C. Han, R. D. Leek *et al.*, 2003 Carbonic anhydrase XII is a marker of good prognosis in invasive breast carcinoma. Br. J. Cancer **88:** 1065–1070.

Wilkinson, M. G., M. Samuels, T. Takeda, W. M. Toone, J. C. Shieh *et al.*, 1996 The Atf1 transcription factor is a target for the Sty1 stress-activated MAP kinase pathway in fission yeast. Genes Dev. **10:** 2289–2301.

Communicating editor: A. P. Mitchell

GENETICS

Supporting Information
http://www.genetics.org/cgi/content/full/genetics.110.118315/DC1

Comparative Transcriptome Analysis of the CO_2 Sensing Pathway Via Differential Expression of Carbonic Anhydrase in *Cryptococcus neoformans*

Min Su Kim, Young-Joon Ko, Shinae Maeng, Anna Floyd, Joseph Heitman and Yong-Sun Bahn

DOI: 10.1534/genetics.110.118315

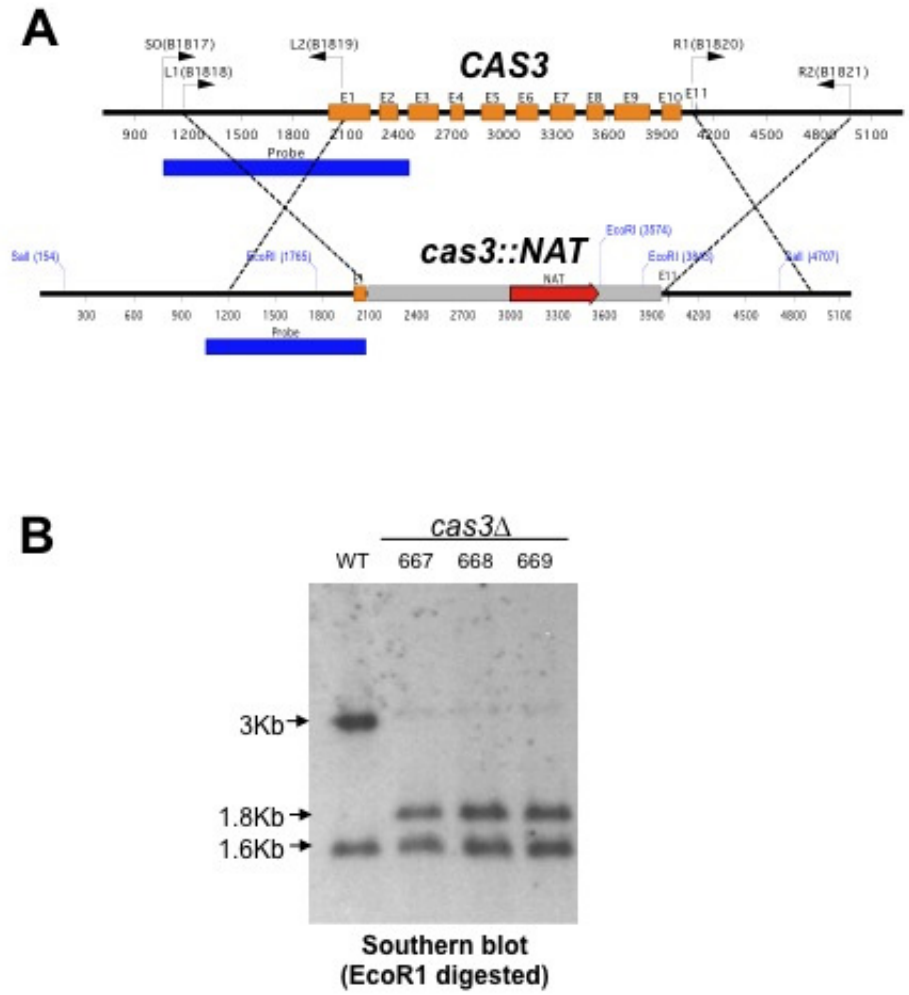

FIGURE S1.—Deletion of the *CAS3* gene. (A) The overlap PCR transformation strategy for disruption of the *CAS3* gene. Primers for overlap PCR and diagnostic PCR are indicated as bent arrows. (D) Southern hybridization was performed to verify positive *cas3Δ* mutants.

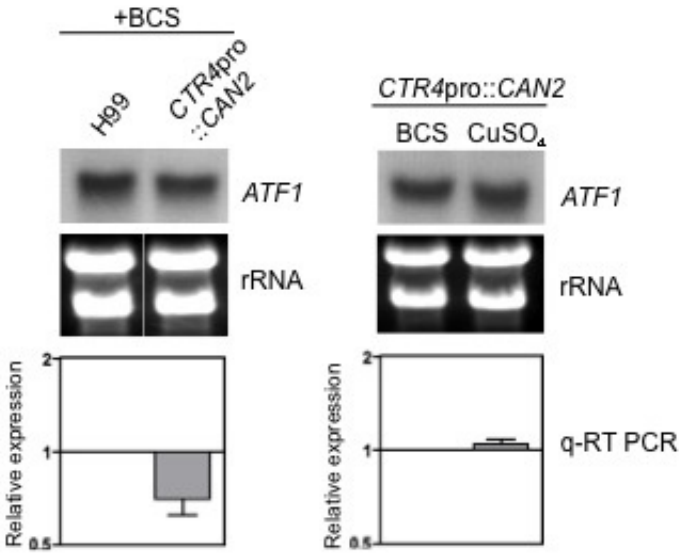

FIGURE S2.—Transcript levels of *ATF1* by overexpression or suppression of *CAN2* expression. Northern blot (top panel) and quantitative RT-PCR (qRT-PCR, bottom panel) show transcript levels of *ATF1* in the wild-type and the P_{CTR4}::*CAN2* strains grown in YNB+BCS medium (left panel) or the P_{CTR4}::*CAN2* grown in YNB+BCS and YNB+$CuSO_4$ medium. For qRT-PCR, data obtained from three independent biological replicates with three technical replicates were normalized by using *ACT1* as a control. Relative gene expression indicates normalized *ATF1* expression levels to those of the wild-type strain (left panel) or the P_{CTR4}::*CAN2* strain in YNB+BCS medium (right panel).

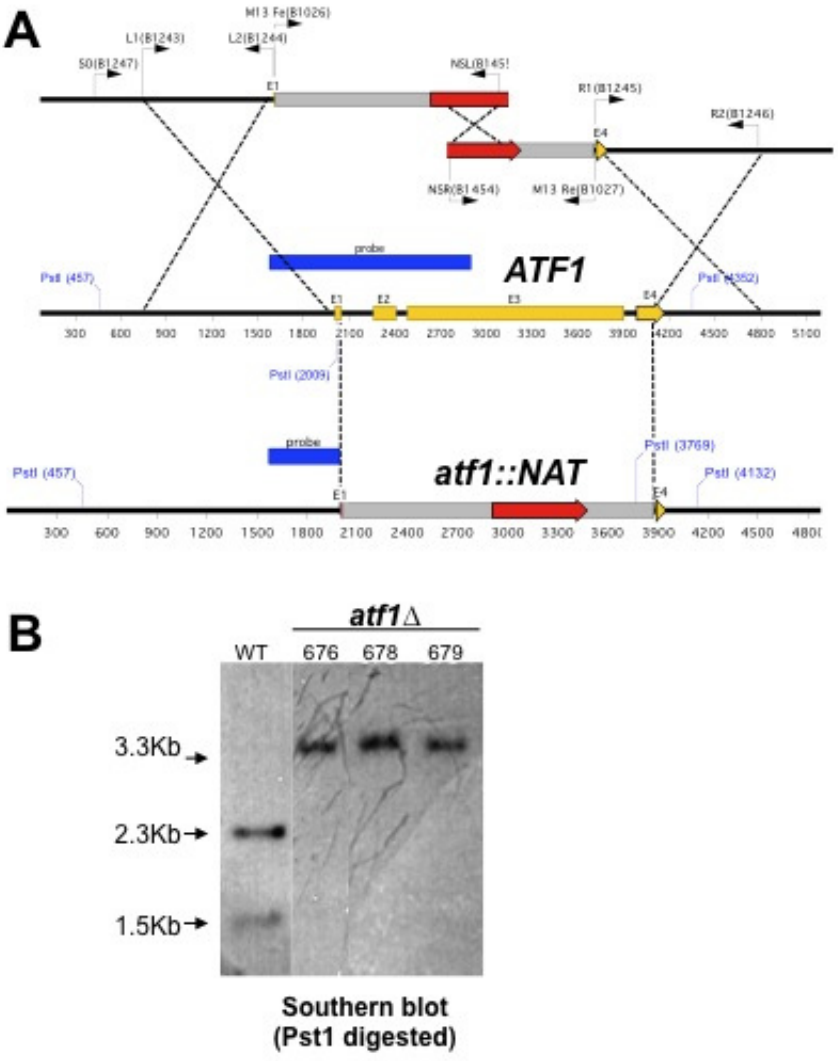

FIGURE S3.—Deletion of the *ATF1* gene. (A) The *NAT* split-marker transformation strategy for disruption of the *ATF1* gene. Primers for the double-joint PCR and diagnostic PCR are indicated as bent arrows. (D) Southern hybridization was performed to verify positive *atf1Δ* mutants.

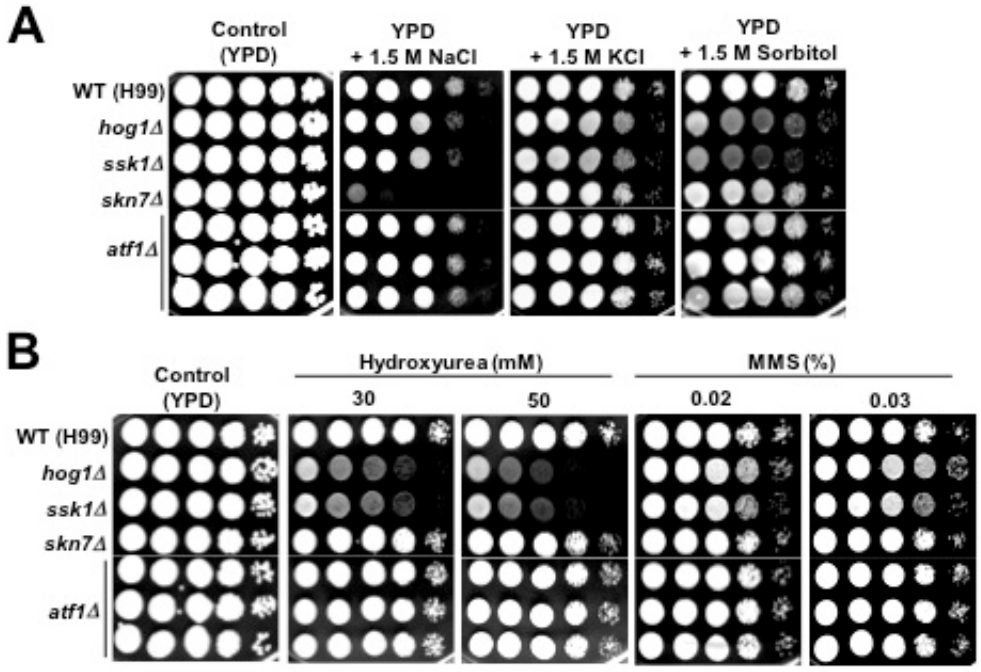

FIGURE S4.—The role of Atf1 in osmotic and genotoxic stress response. Each *C. neoformans* strain (the wild-type H99 strain and *hog1Δ* [YSB64], *ssk1Δ* [YSB261], *skn7Δ* [YSB349], *atf1Δ* [YSB676, YSB678, and YSB679] mutant strains) was grown overnight at 30°C in liquid YPD medium, 10-fold serially diluted ($1–10^4$ dilutions), and spotted (3 μl of dilution) on YPD agar containing the indicated concentrations of NaCl, KCl, sorbitol, methylmethane sulfonate (MMS), and hydroxyurea (HU). Cells were incubated at 30°C for 72 h and photographed.

TABLE S1

***C. neoformans* strains and primers used in this study**

Strain	Genotype	Parent	Reference
H99	*MAT*α		(Perfect *et al.*, 1993)
H99-Eunich	*MAT*α	H99	
BE7-151	*MAT*α *atf1Δ::HYG*	H99-Eunich	
YSB64	*MAT*α *hog1Δ::NAT-STM#177*	H99	(Bahn *et al.*, 2005)
YSB261	*MAT*α *ssk1Δ::NAT-STM#205*	H99	(Bahn *et al.*, 2006)
YSB349	*MAT*α *skn7Δ::NAT-STM#201*	H99	(Bahn *et al.*, 2006)
YSB733	*MAT*α P_{CTR4}::*CAN2*	H99	This study
YSB734	*MAT*α P_{CTR4}::*CAN2*	H99	This study
YSB735	*MAT*α P_{CTR4}::*CAN2*	H99	This study
YSB667	*MAT*α *cas3Δ::NAT-STM*#122	H99	This study
YSB668	*MAT*α *cas3Δ::NAT-STM*#122	H99	This study
YSB669	*MAT*α *cas3Δ::NAT-STM*#122	H99	This study
YSB676	*MAT*α *atf1Δ::NAT-STM*#220	H99	This study
YSB678	*MAT*α *atf1Δ::NAT-STM*#220	H99	This study
YSB679	*MAT*α *atf1Δ::NAT-STM*#220	H99	This study

Primer Name	Sequence	Comment
B79	TGTGGATGCTGGCGGAGGATA	*ACT1* promoter screening oligo
B93	CTATGCTGTAATGACTGAGCC	CAN2 CR2
B354	GCATGCAGGATTCGAGTG	NAT/CTR Left
B355	GATTGGTGAAGTCGTTGTCG	NAT/CTR Right
B356	CATTTCGCTTGCCATAAGTG	CAN2 CSO1
B357	CACCTTCTTGATTGTAGGGG	CAN2 CL1
B358	CACTCGAATCCTGCATGCAAACCCCAACCAACCCCGATTG	CAN2 CL2
B359	CGACAACGACTTCACCAATCATGCCTTTCCACGCTGAACC	CAN2 CR1
B1026	GTAAAACGACGGCCAGTGAGC	M13F extended
B1027	CAGGAAACAGCTATGACCATG	M13R extended
B1243	GAGTAGAGGAGTGGATTGGG	ATF1-L1 for the left flanking region
B1244	GCTCACTGGCCGTCGTTTTACCCATTGTTCAAGCAGAGC	ATF1 L2 for the left flanking region
B1245	CATGGTCATAGCTGTTTCCTGGGCTTACTGCTATCTTGATGC	ATF1 R1 for the right flanking region
B1246	GAAAGAGGAACTACATACTGGGTC	ATF1 R2 for the right flanking region
B1247	GTCTTTTGCTCCTTGAAACC	ATF1 screening oligo paired with B79
B1377	ATTGATTCCAGCAGACCCC	ATF1 southern probe paired with B1780

B1454	AAGGTGTTCCCCGACGACGAATCG	NAT Split marker Right (NSR)
B1455	AACTCCGTCGCGAGCCCCATCAAC	NAT Split Marker Left (NSL)
B1780	ACCAGGTGTAAACCCAGTCC	ATF1 southern probe paired with B1377
B1817	AAAACCTGGGCGGAACACAG	CAS3 screening oligo paired with B79
B1818	CGTCGGACATTCATCAATCTAC	CAS3 L1 for the left flanking region
B1819	GCTCACTGGCCGTCGTTTTACTTGGCAGGAAGAGAGTTATG	CAS3 L2 for the left flanking region
B1820	CATGGTCATAGCTGTTTCCTGGCATAGTGTGGCTGACTTTAG	CAS3 R1 for the right flanking region
B1821	ATGGTCCCACTGCTCACTATCC	CAS3 R2 for the right flanking region
B1829	CCGAAGCCTTTTGTGACTAC	CAS3 southern probe oligo

Each *NAT-STM#* indicates the Nat^r marker with a unique signature tag.

References for Table S1

Bahn, Y.S., Geunes-Boyer, S., and Heitman, J. (2007). Ssk2 mitogen-activated protein kinase kinase kinase governs divergent patterns of the stress-activated Hog1 signaling pathway in *Cryptococcus neoformans*. Eukaryot. Cell *6*, 2278-2289.

Bahn, Y.S., Hicks, J.K., Giles, S.S., Cox, G.M., and Heitman, J. (2004). Adenylyl cyclase-associated protein Aca1 regulates virulence and differentiation of *Cryptococcus neoformans* via the cyclic AMP-protein kinase A cascade. Eukaryot. Cell *3*, 1476-1491.

Bahn, Y.S., Kojima, K., Cox, G.M., and Heitman, J. (2005). Specialization of the HOG pathway and its impact on differentiation and virulence of *Cryptococcus neoformans*. Mol. Biol. Cell *16*, 2285-2300.

Bahn, Y.S., Kojima, K., Cox, G.M., and Heitman, J. (2006). A unique fungal two-component system regulates stress responses, drug sensitivity, sexual development, and virulence of *Cryptococcus neoformans*. Mol. Biol. Cell *17*, 3122-3135.

Idnurm, A., Walton, F.J., Floyd, A., Reedy, J.L., and Heitman, J. (2009). Identification of *ENA1* as a virulence gene of the human pathogenic fungus *Cryptococcus neoformans* through signature-tagged insertional mutagenesis. Eukaryot Cell *8*, 315-326.

Kwon-Chung, K.J., Edman, J.C., and Wickes, B.L. (1992). Genetic association of mating types and virulence in *Cryptococcus neoformans*. Infect. Immun. *60*, 602-605.
Liu, O.W., Chun, C.D., Chow, E.D., Chen, C., Madhani, H.D., and Noble, S.M. (2008).

Systematic genetic analysis of virulence in the human fungal pathogen *Cryptococcus neoformans*. Cell *135*, 174-188.
Perfect, J.R., Ketabchi, N., Cox, G.M., Ingram, C.W., and Beiser, C.L. (1993).

Karyotyping of *Cryptococcus neoformans* as an epidemiological tool. J. Clin. Microbiol. *31*, 3305-3309.

TABLE S2

Microarray data generated by this study

Table S2 is available for download as an Excel file at http://www.genetics.org/cgi/content/full/genetics.110.118315/DC1.

TABLE S3

Genes regulated by differential expression of *CAN2* in the *CAN2* promoter replacement strain growing in either BCS or Copper-containing medium

Table S3 is available for download as a Word (.doc) file at http://www.genetics.org/cgi/content/full/genetics.110.118315/DC1.

TABLE S4

Genes regulated by differential expression of *CAN2* between the wild-type strain and the *CAN2* promoter replacement strain growing in BCS-containing medium

Table S4 is available for download as a Word (.doc) file at http://www.genetics.org/cgi/content/full/genetics.110.118315/DC1.

TABLE S5

List of Can2-dependent genes in *C. neoformans*

Table S5 is available for download as a Word (.doc) file at http://www.genetics.org/cgi/content/full/genetics.110.118315/DC1.